DESIGN AND ANALYSIS OF COMPOSITE PROPELLER BLADES FOR AIRCRAFT

K. Pruthvi Naidu, PG Scholar, JNTUA College of Engineering, Ananthapuramu, INDIA
Email ID: **Pruthvinaidu2903@gmail.com**
Prof. **B.Durga Prasad** Professor & Director of OTPRI, Dept. of Mechanical Engineering., JNTU, Ananthapuramu, INDIA

Abstract:
The numerical prediction approach to assess the performance of small-scale propellers is presented in the current work. FLUENT, a commercially accessible computational fluid dynamics (CFD) solver, is used to carry out the investigation. To identify the difference in the thrust coefficient, power coefficient, and efficiency for an advanced precision composites (APC) Slow Flyer propeller blade, numerical findings are compared with the available experimental data. Unstructured tetrahedron meshing was used throughout the investigation along with a typical k-! turbulence model. The propeller's rotation at 3008 revolutions per minute (RPM) towards its local reference frame was also taken into account using the Multiple Reference Frame approach. Catia V5 R20 was used to create the model, while CFD Fluent 16.0 was used for analysis.Keywords: APC slow flyer, CFD, propeller, blade, Catia V5 R20,CFD 16.0.

1. Introduction

When compared to the cross-section of an aeroplane wing, a propeller can be thought of as a revolving wing that assembles airfoils. A fundamental propeller layout has a minimum of two blades joined at the hub [1]. The engine's rotational power is converted into thrust to propel the aircraft forward through the air. The airflow in front of the blade moves more quickly due to the airfoil's chamber shape.
According to Bernoulli's principle, the airflow is accelerated, which results in a decrease in static pressure in front of the blade. The propeller also experiences increased static pressure at the back because of the lower speed there. The response force pulls the aeroplane forward as a result of the decreased pressure at the front. It is possible for an aeroplane to overcome drag thanks to the thrust force produced by the pressure differential between the front and back sections of the propeller [2].
Numerous methods, including experimental investigation and numerical analysis, may be used to determine the performance of a propeller. In the experimental technique, the propeller blade is tested in a wind tunnel under both static and progressive flow conditions. Three-dimensional computational fluid dynamics (CFD) simulation uses the Reynolds-average Navier-Stokes (RANS) equation for numerical analysis. The use of CFD technologies in propeller design and analysis has grown significantly.
Using either of the two ways, the propeller's performance for full-scale conventional aircraft has been well-documented, but little research has been done on small-scale and low Reynolds number propellers [3].
Unmanned aerial vehicles (UAVs) typically use propellers that are tiny in diameter, operate at low Reynolds numbers, and have slow tip speeds [4]. Based on the chord at the 75% span point, the Reynolds number taken into account in this study is fewer than 100,000 [3, 5]. Over the past few decades, there has been a substantial surge in the development and use of UAVs [4]. In order to be sure that the design has produced a trustworthy UAV performance, it is crucial to look into the propeller performance.
Numerous designs have developed since the invention of using aircraft propellers to keep up with the quick development of aeronautical technologies. There are numerous propeller designs available to accommodate different mission profiles for aeroplanes. The goal of propeller advances in airfoil selection, The quest of a highly efficient propeller performance includes blade twist, blade angle, and propeller diameters. Most of the modification parameters are focused on the typical propeller blade design, which includes a large-scale propeller used in typical aircraft.
smaller than 24 inches, using a lower Reynolds number, moving more slowly in the forward direction, and having a higher RPM are characteristics of propeller blades with an unorthodox design [4]. Due

to the small number of tests and lack of established techniques for studying propeller performance, the dependability of the unorthodox design is still questionable.
The current study's goal is to provide an in-depth analysis of one method for determining how well a propeller blade will function while it is running at a low Reynolds number. The current study's objective is to compute the thrust coefficient, power coefficient, and efficiency while adjusting the advance ratio by simulating the flow of a propeller blade using CFD software (FLUENT). This paper presents a tried-and-true technique and setup capable of estimating propeller performance using CFD Fluent, hence eliminating the need for further research to carry out a CFD setup study and validation prior to assessing a new propeller design.

Literature review

Due to the small number of tests and lack of established techniques for studying propeller performance, the dependability of the unorthodox design is still questionable.
The current study's objective is to provide a comprehensive analysis of one method for determining a propeller blade's performance when it is operating at a low Reynolds number. In order to compute the thrust coefficient, power coefficient, and efficiency while adjusting the advance ratio, the current study aims to model the flow of a propeller blade using CFD software (FLUENT). This paper provides an established approach and setup capable of forecasting propeller performance using CFD Fluent, hence removing the need for further research to carry out a CFD setup study and validation prior to studying a new propeller design.
The similar technique was applied by Deters et al. [3] using a different kind of propeller blade. 27 small-scale propellers were put to the test, and data on thrust, power, and propeller efficiency were gathered for a specific range of advance ratios. Since aerodynamic performance factors like lift and drag are more noticeable at Reynolds numbers below 100,000, the studies were designed to explore the impacts of Reynolds number on a small-scale propeller. As the Reynolds number rose, the performance of the propellers improved, according to the results.
To ascertain the performance of a propeller blade operating at a Reynolds number of 30,000 to 300,000, Merchant [6] also carried out an experimental method investigation. For applications requiring low Reynolds numbers, the experimental technique used in the paper is successful in producing accurate data sets. CFD is one of the most effective technologies for determining flow properties, hence it was employed in some investigations.
By using CFD analysis, Subhas et al. [7] carried out a study on the ship propeller flow.
In the beginning, the geometry was created in CAD software using precise propeller dimensions and blade angles. The flow domain was assumed to be a cylinder enclosure, with the inlet located 3D (where D is the diameter of the propeller blade) away from the blade and the exit located 4D downstream of the same position. The entire flow domain and propeller were mesh-generated. The work used a moving reference frame and the k-" turbulence model. When experimental findings and data on thrust and torque coefficients from CFD are compared, they match up well. The study comes to the conclusion that CFD analysis may reasonably forecast flow characteristics.
Additionally, Wang et al.'s [8] investigation of marine propeller performance for CFD analysis using transition sensitive turbulence modelling. By integrating transitional analysis, the study offers a way to reduce the difference between CFD and experimental data. According to the study, the results were superior to the k-! SST (Shear Stress Transport) turbulence model in terms of propeller forecast accuracy.
For the purpose of making numerical forecasts of a maritime propeller, Morgut et al. [9] investigated the effects of the grid type and turbulence model choice. To research the effects of the meshes, hexa-structured and hybrid unstructured meshes were compared during meshing. Additionally, it was investigated how accurate SST and BSL-RSM (Baseline Reynolds Stress Model) were. Both meshes in the investigation showed a similar level of accuracy, and BSL-RSM offers marginally better accuracy than SST with longer computing times.
Benini [10] compared the approaches for estimating the performance of the propeller blade, including the combined momentum-blade element theory and fully three-dimensional numerical RANS using

CFD Fluent. The results show that, regardless of the advance ratio, the numerical approach utilised delivers results that are reliable with a maximum discrepancy of 5% when compared to experimental data. In terms of results, the numerical analysis performs better than the combined momentum-blade element theory.
Morgado et al. [11,12] developed a novel propeller and an analytical method that can evaluate a propeller's performance. The programme uses an enhanced blade element momentum for each blade segment. The outcomes were validated using experimental data taken from the National Advisory Committee for Aeronautics (NACA) Technical Report. To build and optimise a new propeller, the software's capabilities are put to the test once again [13].

2. Methodology

The propeller used in UAVs typically has a diameter of less than 24 inches. Due to its widespread use in UAVs and the availability of experimental data, the advanced precision composites (APC) Slow Flyer propeller is chosen as the reference design in the current study [14].

Table 1. Simulation flow conditions.

In Section 3, there are further specifics on the APC Slow Flyer.CATIA V5 R20 was used for the design. Utilising ANSYS Inc.'s commercially available CFD solver FLUENT 15.0, this propeller's

Advance Coefficient, J	Free Stream Velocity (m/s)
0.192	2.4384
0.236	2.9972
0.282	3.5814
0.334	4.2418
0.383	4.8641
0.432	5.4864
0.486	6.1722
0.527	6.6929
0.573	7.2771
0.628	7.9756
0.659	8.3693
0.717	9.1059
0.773	9.8171
0.799	10.1473

numerical simulation is carried out. To evaluate the CFD method used to extract the propeller performance parameters, the numerical analytical results are compared with experimental data [3,14].

3. Propeller Model using Catia

Two-bladed, 0.254 m in diameter, and with a fixed pitch, the APC Slow Flyer has a propeller. The propeller is made up of narrow airfoil profiles with a particular arrangement of a Clark-Y airfoil near the tip [15] and a low Reynolds number Eppler E63 airfoil, inserted to form a sharp leading-edge blade design, as seen in Figure.

Figure 1. Standard APC Slow Flyer 10 inches x 7 inches propeller blade.

The pitch of 0.1778 m provides a pitch-to-diameter ratio of 0.7, which is normal for an off-the-shelf propeller type. With a chord at a 75% blade station and a rotational speed of 3008 RPM, the propeller has a Reynolds number of around 50,804 (RPM). The APC Slow Flyer used in this experiment, shown in Figure 1, is modelled using CAD software prior to analysis in FLUENT 15.0.

4. Numerical Setup

The setup used in the numerical analysis is further explained in this section.

4.1 Flow Domain

The commercial CFD solver ANSYS FLUENT 15.0 was used to carry out the numerical forecasts made in this investigation. The flow around the propeller was predicted numerically using the Multiple Reference Frame model (MRF) method. Figure 2a defines and exemplifies the domain. The domain is separated into a broad stationary zone known as the global domain and a narrow rotating region known as the rotating domain. As seen in Figure 2b, a smaller cylinder completely surrounding the hub and blades defines the spinning domain.

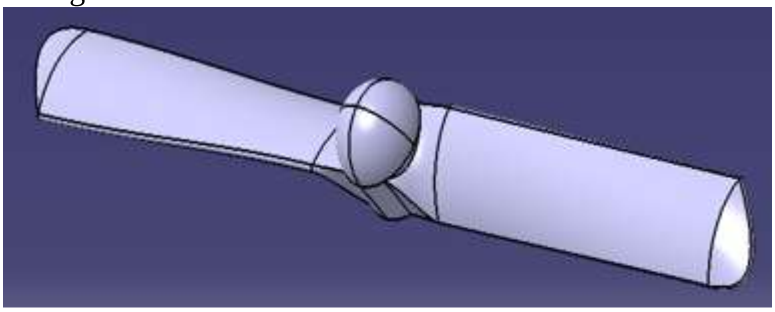

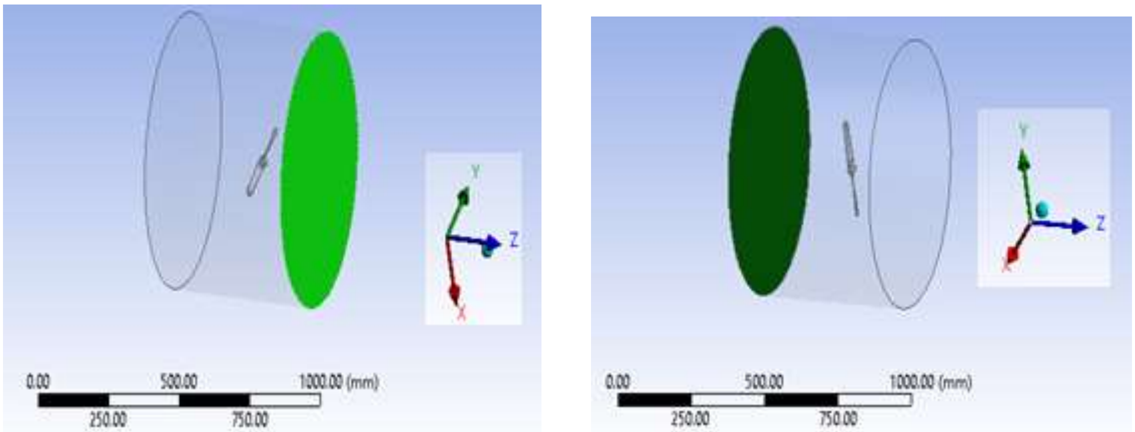

Fig2. Inlet & outlet

The inlet, outflow, and outer boundary of the stationary zone are positioned far enough from the propeller to prevent the full development of the upstream and downstream flow from influencing the results of the research. Both above and downstream of the propeller's origin, in position 4D, are the boundaries of the inlet and outflow. The enclosure is set up for the spinning domain to be 1.1D and 0.4D. The upstream and downstream lengths of the flow domain must be carefully chosen in order to prevent recirculation of the flow, which will cause convergence problems.

4.2 Mesh Generation

The grid was made using Fluent 15.0's mesh tool. The grid is important because it provides a distinctive representation of the pertinent geometry. The performance of the numerical analysis, the convergence rate, and the computation time for the analysis were all directly influenced by the computational grid's quality. In order to conduct the current investigation, the mesh's cell sizes were designed to be smaller along the blade in the spinning region and increasingly bigger towards the stationary area. By ensuring that the grid improvements are distributed evenly over the interface, the accuracy of the results is increased. complex geometries with minimal to no human interaction. Table 2 presents the information for mesh grid creation. It is simpler to adapt the grid to the physical solution—that is, to refine or coarsen the grid—on an unstructured grid than on a structured grid.

TABLE 2
Mesh

Object Name	*Mesh*
Defaults	
Physics Preference	CFD
Solver Preference	Fluent
Relevance	0
Nodes	199308
Elements	273911
Mesh Metric	None

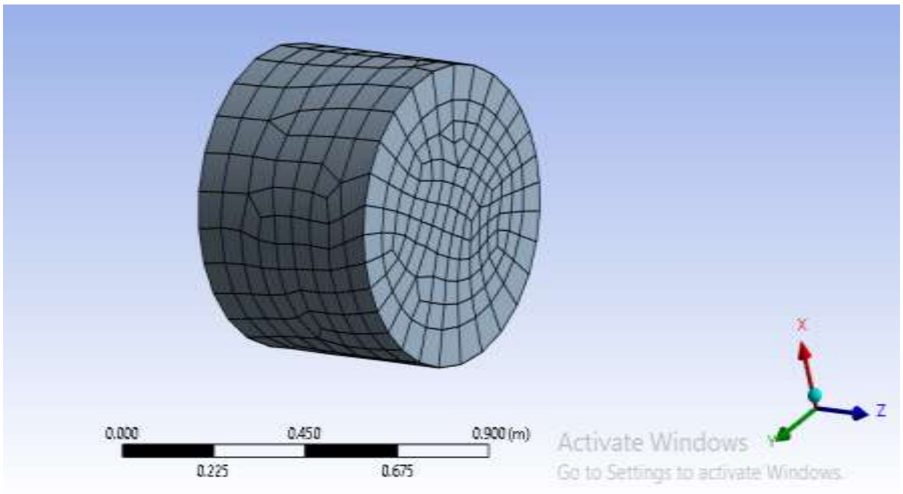

Fig3. Mesh

4.3 Boundary Conditions

CFD simulations were performed under the flow parameters stated in Table 1 with a fixed rotational speed of 3008 RPM. At the intake boundary, the free-stream velocity with a 0.1% turbulence intensity is stated. The turbulence intensity is chosen based on data of wind tunnel intensity made by [3,5,14]. Outflow boundary conditions were created at the flow exits that are located below the flow domain. There is a no-slip rule posted on the walls. It is the responsibility of the MRF to include the rotational speed in the region that encompasses the propeller blade.

The approach is particularly suited to the analysis, which requires the interaction between fixed and rotating frames. There will be a certain rotational or translational speed assigned to each zone. A local frame transformation will be made to the interface between the two zones to enable the usage of the flow variable from one zone by the neighbouring zones. The rotating reference frame is given a rotational speed of 3008 RPM. With reference to the cell zone adjacent to it, the wall that serves as both the hub and the propeller blade was likewise given the spinning feature.

Pressure and velocity are coupled via the Semi-Implicit Method for Pressure-Linked Equations (SIMPLE). The Second Order Upwind method was used for velocity and pressure. The gradients were calculated using the Least Square Cell-based Algorithm and the First Order Upwind for Turbulent Kinetic Energy and Turbulent Dissipation Rate. First order algorithms generated accurate findings for this experiment.

5. Results and Discussions

The outcomes of the numerical analysis were compared with experimental data that was previously available in order to verify the grid's influence and the accuracy of the data gathered. For all computer computations, the force and momentum were resolved in a three-coordinate system with the values x, y, and z. The axial force and momentum around the propeller axis, respectively, determine the thrust and torque.

T (N) denotes thrust, Q (Nm) denotes torque, n (rps) denotes propeller rotation speed, D (m) denotes propeller diameter, and r (kg_m-3) denotes fluid density in these equations. The relative percentage inaccuracy of the torque coefficient, KQ, and thrust coefficient, KT, may be calculated using equations (4) and (5) as shown below.

$$K_T = T/\rho n^2 D^2 \text{........(1)}$$
$$KQ = Q/\rho n^2 D^5 \text{......(2)}$$
$$KP = P/\rho n^3 D^5 \text{.......(3)}$$
$$\Delta K_T(\%) = K_{TCFD} - K_{TEXP}/\ K_{TEXP} \text{ X } 100\ldots(4)$$
$$\Delta K_Q(\%) = K_{QCFD} - K_{TEXP}/\ K_{QEXP} \text{ X } 100\ldots(5)$$
$$J = V/nD \text{..........(6)}$$
$$\eta = K_T\ J/K_P \text{.......(7)}$$

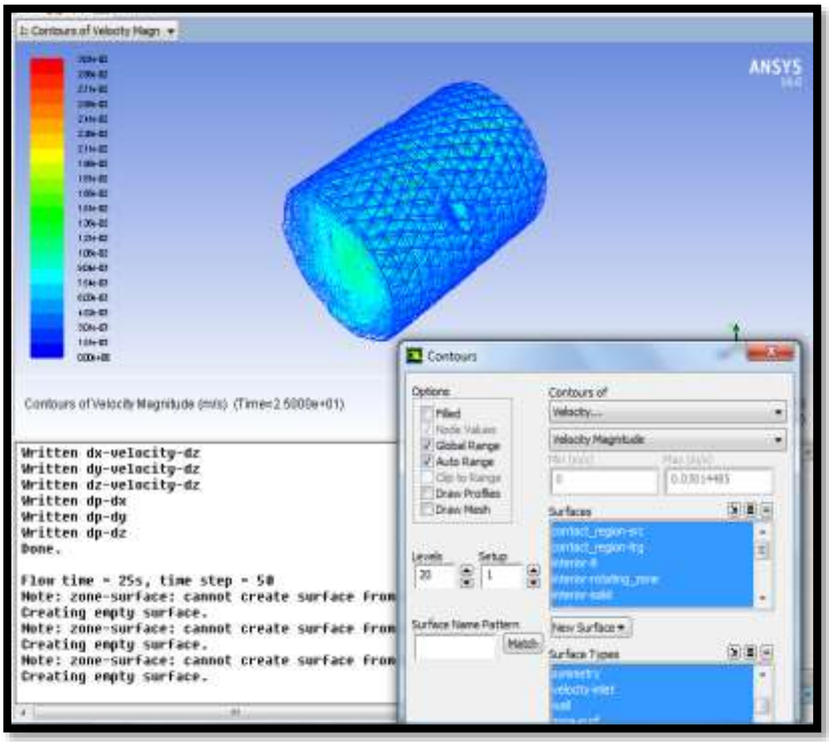

Fig4: Velocity magnitude

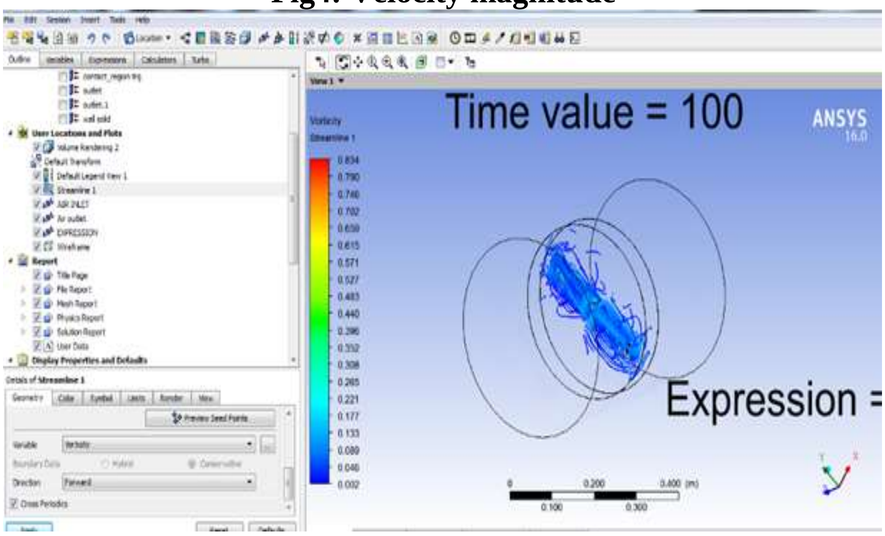

Fig5. Velocity in inlet region

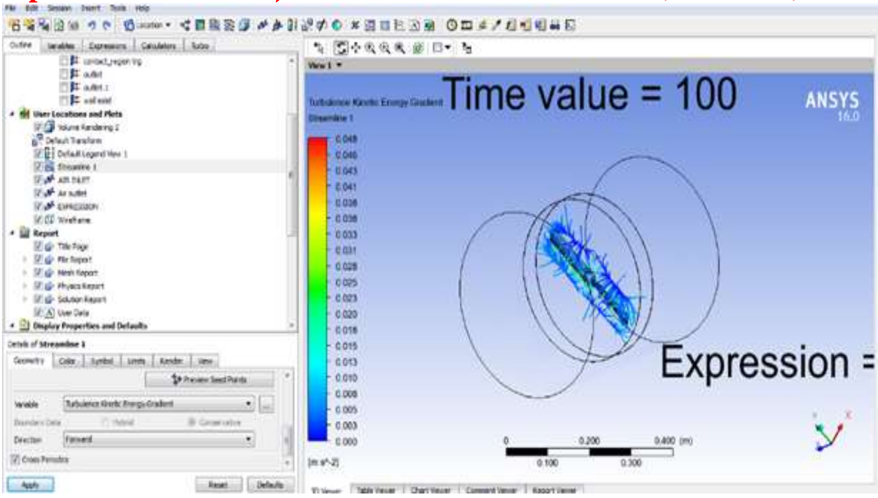

Fig6. Inlet Turbulence Kinetic

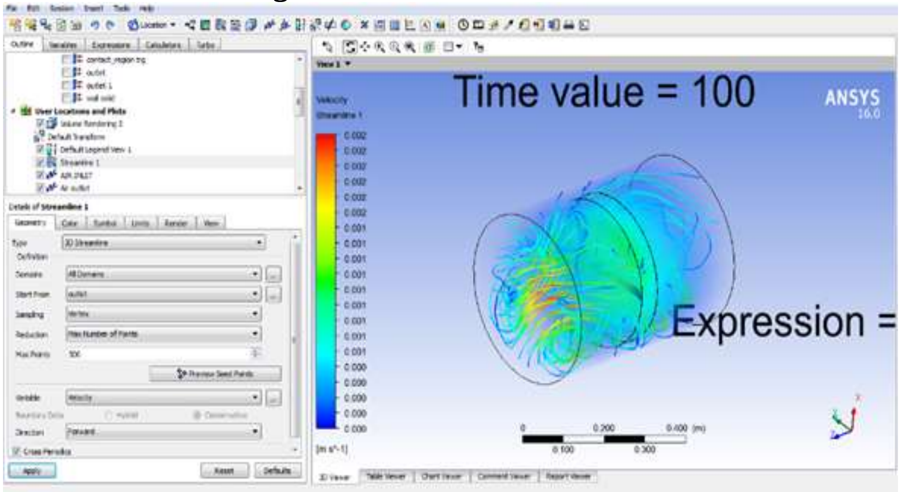

Fig7. Velocity in Outlet region

Figure 8 depicts the propeller blade's pressure profile when it is operating at an advance ratio of J = 0.628. The illustration shows that the pressure on the propeller's rear side is obviously higher than the pressure on its front side. Similar to an aviation wing, the pressure differential between the top and bottom surfaces of the wing creates the lift force required for flight. The pressure difference between the propeller's front and rear surfaces creates the thrust when it comes to propellers.

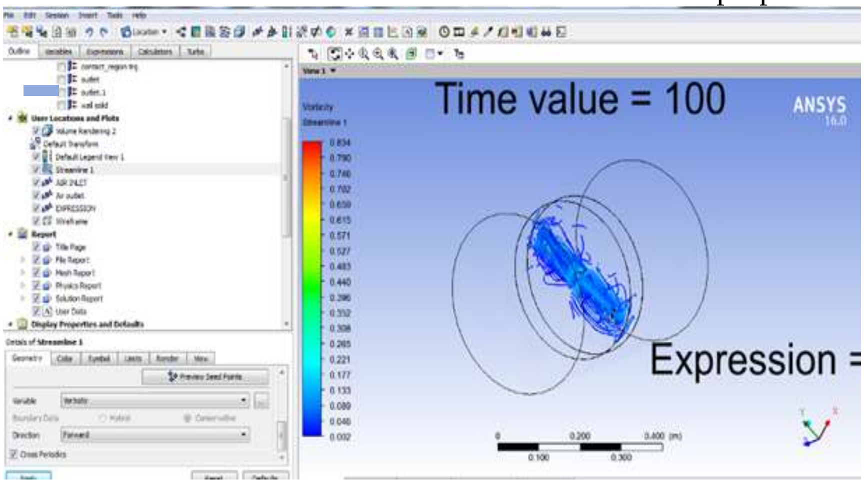

Figure 8. Propeller blade pressure contour for J = 0.628. (Top) Front-side of the propeller;

Conclusions

The experimental results were successfully duplicated by the CFD simulations utilised in this study, which may greatly increase computational accuracy. As a result of the current study, it is now possible to evaluate various propeller blade configurations and get trustworthy data for small-scale, low

ISSN: 2278-4632
Vol-13, Issue-05, No.02, May : 2023

Reynolds number propellers. Commercial CFD software, like FLUENT, has been proven to be trustworthy in making accurate preliminary predictions; as a result, it can take the place of experimental analysis, which is time-consuming and more expensive. The approach suggested in this work makes use of both a multiple reference frame model and a typical k-turbulence model to account for the rotating influence of the propeller blade. The mesh independent research looked at the error and computation time required for decision-making, as well as the effects of the final meshing number on the overall domain. The results for the thrust coefficient indicated a small under-prediction for a low advance ratio, but the results for the power coefficient show both an under-prediction for a low advance ratio and an over-prediction for a greater advance ratio. Efficiency was good across the advance ratio, with the exception of a little overprediction on the higher advance ratio. Overall findings indicated a solid capacity to forecast a small-scale propeller's performance at low speeds and low Reynolds numbers.

References

1. Delp, F. Aircraft Propellers and Controls, 1st ed.; Jeppesen: Frankfurt, Germany, 1979.
2. Watts, H.C. The Design of Screw Propellers: With Special Reference to Their Adaptation for Aircraft, 1st ed.; Forgotten Books: London, UK, 1920.
3. Deters, R.W.; Krishnan, G.K.A.; Selig, M.S. Reynolds number effects on the performance of small-scale propellers. In Proceedings of the 32nd AIAA Applied Aerodynamics Conference, Atlanta, GA, USA, 16–20 June 2014; pp. 1–43.
4. Venkatesh, B.J. Design and Performance Evaluation of a Propeller; LAP LAMBERT Academic Publishing GmbH & Co. KG: Saarbrücken, Germany, 2012.
5. Brandt, J.B.; Selig, M.S. Propeller Performance data at low reynolds numbers. In Proceedings of the 49th AIAA Aerospace Sciences Meeting, Grapevine, TX, USA, 7–10 January 2013; pp. 1 18.
6. Merchant, M.P. Propeller Performance Measurement for Low Reynolds Number Unmanned Aerial Vehicle Applications; Wichita State University: Wichita, KS, USA, 2004.
7. Subhas, S. CFD analysis of a propeller flow and cavitation. Int. J. Comput. Appl. **2012**, 55, 26–33.
8. Wang, X.;Walter, K.S. Computational analysis of marine-propeller performance using transition sensitive turbulence modeling. J. Fluids Eng. **2012**, 134, 071107.
9. Morgut, M.; Nobile, E. Influence of grid type and turbulence model on the numerical prediction of the flow around marine propellers working in uniform inflow. Ocean Eng. **2012**, 42, 26–34.
10. Ernesto Benini, Ã. Significance of blade element theory in performance prediction of marine propellers. Ocean Eng. **2004**, 31, 957–974.
11. Morgado, J.; Silvestre, M.Â.R.; Páscoa, J.C. Validation of new formulations for propeller Analysis. J. Propuls. Power **2015**, 31, 467–477.
12. Morgado, J.; Silvestre, M.A.R.; Páscoa, J.C. A comparison of post-stall models extended for propeller performance prediction. Aircr. Eng. Aerosp. Technol. **2016**, 88, 540–549.